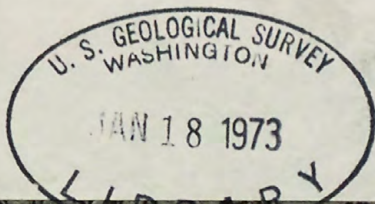


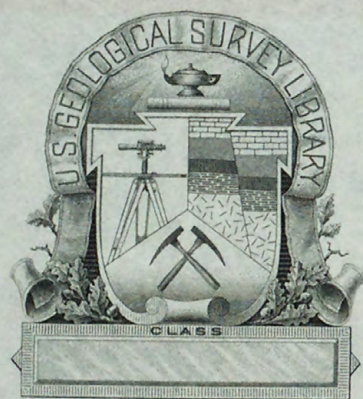
U. S. Geological Survey.

REPORTS-OPEN FILE SERIES, no.1016: 1968.



(200)  
R29o  
no. 1016







(200)  
R290  
[no. 1016]

U. S. Geological Survey. [Report -  
Open file series]

UNITED STATES  
DEPARTMENT OF THE INTERIOR  
GEOLOGICAL SURVEY



sl  
cm  
tw anal

INTERAGENCY REPORT NASA-103  
IMAGERY OF CRATERS PRODUCED BY MISSILE IMPACTS

by

*entry 1928-*  
H. J. Moore, II

Reuben Kachadoorian, *1921-*

and

*shw paces*  
J. F. McCauley, *1922*

268045

U. S. Geological Survey  
OPEN FILE REPORT

This report is preliminary and has  
not been edited or reviewed for  
conformity with Geological Survey  
standards or nomenclature.

U. S. GEOLOGICAL SURVEY  
Washington, D. C.  
20242



For release APRIL 1, 1968

The U. S. Geological Survey is releasing in open files the following reports. Copies are available for consultation in the Geological Survey Libraries, 1033 GSA Bldg., Washington, D.C. 20242; Bldg. 25, Federal Center, Denver, Colo. 80225; and 345 Middlefield Rd., Menlo Park, Calif. 94025. Copies are also available for consultation in other offices as listed:

1. Lithologic logs of six exploratory holes (UCe-9, -10, -11, -12a, -13, and -14) drilled in alluvium in central Nevada, by G. S. Corchary. 19 p., 1 fig., 6 tables. 1012 Federal Bldg., Denver, Colo. 80202; 504 Custom House, San Francisco, Calif. 94111; 7638 Federal Bldg., Los Angeles, Calif. 90012; 8102 Federal Office Bldg., Salt Lake City, Utah 84111; Library, Mackay School of Mines, University of Nevada, Reno, Nev. 89507.
  2. Preliminary materials map of the Woronoco quadrangle, Massachusetts, by G. William Holmes. 1 map (scale 1:24,000), 8 data sheets. Massachusetts Dept. of Public Works, 100 Nashua St., Boston, Mass. 02114; and USGS, 80 Broad St., Boston, Mass. 02110. Material from which copy can be made at private expense is available in the USGS Boston office.
  - ✓ 3. Imagery of craters produced by missile impacts, by H. J. Moore, Reuben Kachadoorian, and J. F. McCauley. 38 p., 17 figs., 1 table. 601 E. Cedar Ave., Flagstaff, Ariz. 86001.
  4. Principal facts for gravity stations in northeastern Washington, by W. E. Davis, and W. T. Kinoshita. 14 p. 504 Custom House, San Francisco, Calif., 94111; 7638 Federal Bldg., Los Angeles, Calif. 90012; 678 U.S. Court House Bldg., Spokane, Wash., 99201; Washington Division of Mines and Geology, Dept. of Natural Resources, 335 General Administration Bldg., Olympia, Wash. 98501.
- The following four reports are available for consultation in the three U. S. Geological Survey Libraries listed in opening paragraph above, as well as at the Kentucky Geological Survey, 307 Mineral Industries Bldg., University of Kentucky, Lexington, Ky. 40506; and USGS, 710 West High St., Lexington, Ky. 40508. Material from which reproduction can be made at private expense is available in the Lexington office of USGS.
5. Preliminary structure map of the Ford quadrangle, central Kentucky, by D. F. B. Black. 1 map, scale 1:24,000.
  6. Preliminary structure map of the Salvisa quadrangle, central Kentucky, by Earle R. Cressman. 1 map, scale 1:24,000.
  7. Preliminary structure map of the Nicholasville quadrangle, Jessamine and Fayette Counties, Kentucky, by W. C. MacQuown. 1 map, scale 1:24,000.
  8. Preliminary structure map of the Little Hickman quadrangle, central Kentucky, by Don E. Wolcott. 1 map, scale 1:24,000.



## CONTENTS

	Page
Abstract -----	1
Introduction -----	2
Experimental Procedure -----	3
Description of craters -----	13
Experimental results	
Comparison of imagery with surface mapping -----	17
Comparison of infrared imagery and measured temperatures -----	29
Explanation of results -----	35
Conclusions -----	37
Future Studies -----	37
References-----	38

## TABLES

Table 1. Time of formation, sizes and experimental conditions for missile impact craters -----	6
--	---

## ILLUSTRATIONS

Figure 1. Map of Crater 36 showing locations of areas where surface temperatures were measured. Scale: 1 inch = 10 feet -----	8
Figure 2. Map of Crater 38 showing locations of areas where surface temperatures were measured. Scale: 1 inch = 10 feet -----	9
Figure 3. Photograph showing thermometers placed in south wall of Crater 38 -----	10
Figure 4. Photograph showing thermometer placed in north wall of Crater 38 -----	11



## CONTENTS (Continued)

Figure 5.	Photograph showing thermometers placed in ejecta near west rim of Crater 38. Note shadows cast by large fragments -----	12
Figure 6.	Photograph showing Crater 37, ejecta and fallout -----	15
Figure 7.	Photograph showing Crater 38, ejecta and fallout -----	16
Figure 8.	Comparisons between surface maps and imagery for Craters 18 and 28 -----	18
Figure 9.	Comparisons between surface maps and imagery for Craters 29 and 30 -----	20
Figure 10.	Comparison between surface maps and imagery for Craters 36, H and 35 -----	22
Figure 11.	Comparison between surface map and imagery for Crater 37 -----	24
Figure 12.	Color (upper) and black-white (lower) imagery of Crater 37, ejecta and fallout -----	25
Figure 13.	Comparisons between surface map and imagery for Crater 38 -----	27
Figure 14.	Color image of Crater 38, ejecta and fallout -----	28
Figure 15.	Time-temperature variations for Crater 36 -----	31
Figure 16.	Time-temperature variations for Crater 38. 14 March 1967, 10:00 - 22:00 hours -----	32
Figure 17.	Time-temperature variations for Crater 38. 15 March 1967, 08:00 - 14:00 hours -----	33



## Imagery of Craters Produced by Missile Impacts

by H. J. Moore, II, Reuben Kachadoorian and J. F. McCauley

### ABSTRACT

Infrared, ultraviolet, color, and black-white imagery of craters produced by missile impacts are useful in the study of distributions of ejecta and fallout from the craters. Detection of ejecta and fallout from the craters with infrared imagery (8-14 microns) is markedly influenced by the local topography but under optimum conditions the ejecta and fallout are shown exceedingly well as relatively cool areas on daytime imagery. The ejecta and fallout may also be detected using ultraviolet imagery (0.345-0.355 microns) but boundaries between ejecta, fallout, and the surroundings are diffuse. Color (0.38-0.78 microns) and black-white (0.45-0.71 microns) photographic imagery effectively show the distribution of ejecta in layered targets and under some conditions ejecta and fallout are also well shown. Color photography is superior to black-white photography in detection of ejecta and fallout distributions. This superiority is also evident in the black-white prints made from color transparencies which are included in this report.



## Introduction

A study of craters produced by missile impacts is being conducted by the U. S. Geological Survey and the Commanding General of White Sands Missile Range. This report describes the results of an analysis of infrared, ultraviolet, color, and black-white imagery of some nine craters of varying size and age. The imagery was obtained by the Earth Resources Program Remote Sensing Aircraft operating from the Manned Spacecraft Center (NASA) in Houston, Texas.



### Experimental procedure

In mid-March 1967, night-time and daylight flights were made by the NASA Remote Sensing Aircraft at altitudes 1,500 to 4,000 feet above nine missile impact craters. The night flights to obtain infrared imagery were between 19:45 and 20:15 hours (local time) on 14 March at about 1,500 feet above the craters. Sundown occurred at 18:05 and sunset was 18:30. The daylight flights were between 09:05 and 10:10 hours (local time) on 15 March at about 1,500 and 5,000 feet to obtain imagery with the Reconafax IV infrared scanner (8 to 14 microns), ultraviolet camera (0.345 to 0.355 microns), RC 8 camera with color Ektachrome film (0.38 to 0.78 microns) and the T-11 camera with Plus-X film (0.45 to 0.71 microns). Radar and radiometers were also in operation but data from these instruments have not been requested at this time. The scales of the imagery are: (1) infrared near 1:22,500; (2) ultraviolet near 1:70,000, and (3) photographic near 1:3,000. Ground speeds of the aircraft ranged between 150 and 192 knots. A flight summary report for Mission 43, site 14 (NASA, 1967) contains the details of the flights and the operation of the remote sensing equipment.

The results and preliminary interpretations of a previous remote sensing experiment in July 1966 have been reported (Moore and others, 1967). Flight data are contained in a flight summary report for Mission 28 (NASA, 1966). It is noteworthy that imagery of three of the craters in



the 1966 experiment were obtained within several hours of impact between 14:00 and 15:00 and that local rain showers may have affected the results.

Outlines of the images were prepared by visual inspection of infrared positive transparencies, ultraviolet, color, and black-white transparencies.



Plane table topographic and geologic maps of the craters were prepared at scales between 1/24 and 1/500 for use in comparing ground observations with the imagery. The ages of the craters mapped range from a few days to at least several years (see table 1). For Mission 43 (March, 1967), imagery of two craters was obtained within two days of formation; two were about one week old; three were about 8 months old; one was 21 months old; and one was at least several years old.

Data on the surface and subsurface temperatures of two craters were obtained using a Barnes Radiometer which measures infrared radiation (in the 8-14 micron wavelength band) and Weston stem thermometers. Temperature data were collected about 1 week prior to the flights for crater 36 and during the flights for crater 38. Air temperatures in the shade were obtained using a standard bulb thermometer. Calibration of the thermometers using hot and cold water showed the Weston thermometers agreed within  $1^{\circ}$  or less at  $48^{\circ}\text{C}$ , within  $0.5^{\circ}$  at  $22^{\circ}\text{C}$ , and  $1.5^{\circ}$  or less at  $12^{\circ}\text{C}$ . A maximum difference of  $3^{\circ}$  was noted at  $37^{\circ}\text{C}$ . Bulb temperatures were about  $1^{\circ}$  to  $2^{\circ}$  higher than those of the Weston thermometers. Radiometer temperatures agreed within  $2.5^{\circ}$  of the bulb thermometer and were always less. The radiometer read  $-2^{\circ}\text{C}$  for ice cubes.

Table 1.--Time of formation, sizes, and experimental conditions for missile impact craters.

	Date made	Diameter (ft.)	Depth (ft.)	Kinetic Energy (ergs)	Angle of impact
Crater 18	June 1965	20.1-21.2	5.2	$2.4 \times 10^{15}$	46°
Crater 28	July 1966	17.2-18.0	4.4	$1.6 \times 10^{15}$	47°
Crater 29	July 1966	18.0-16.2	3.4	$1.6 \times 10^{15}$	47°
Crater 30	July 1966	14.0-14.4	3.5	$1.6 \times 10^{15}$	47°
Crater 36	March 1967	14.8-18.2	3.2	$1.4 \times 10^{15}$	48°
Crater 37	March 1967	16.4-18.6	2.9	$1.6 \times 10^{15}$	47°
Crater 38	March 1967	18.8-18.8	4.0	$1.6 \times 10^{15}$	47°
Crater H	Several years ago	≈45	≈10	unknown	unknown



Temperature readings were taken about every hour at selected points in and around the craters. Location of sites where Barnes Radiometer readings were taken for crater 36 on 7 March 1966 are shown in figure 1. Loose connections in the head of the radiometer caused sporadic readings but prior to each reading, operator hand temperatures were taken to test instrument stability. Only four Weston stem thermometers were available when the temperatures of crater 36 were taken and these were implaced within 1.5 hours after impact. Thermometer stations coincided with the following Barnes Radiometer stations (fig. 1): (1) south wall, (2) ejecta, (3) plane table, and (4) the northern-most control station. All of the Weston thermometers had 8-inch stems and were inserted the full 8 inches except at the north control station, where the stem was inserted only 5 inches. Seven Weston thermometers were available for crater 38 on 14 and 15 March. Four were buried 8 inches alongside of four at 4 inches at the following radiometer stations shown in figure 2: (1) south wall, (2) ejecta rim west, and (3) the western-most control station. One Weston thermometer was buried 8 inches on the north wall. The details of the thermometer stations are shown in figures 3, 4, and 5. All air temperatures were obtained with the bulb thermometer.

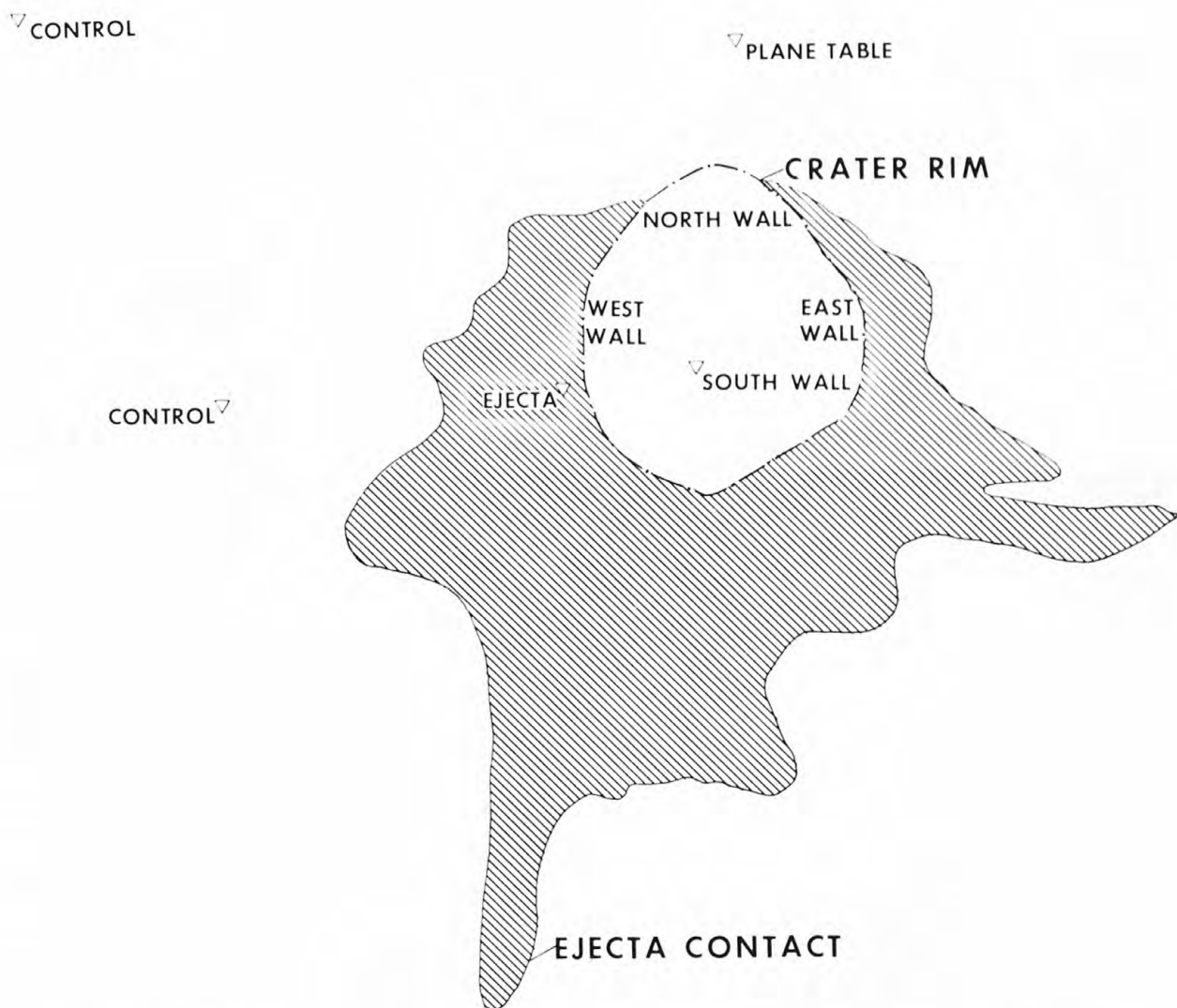


Figure 1. Map of crater 36 showing locations of areas where surface temperatures were measured.  
Scale: 1 inch = 10 feet



CONTROL ▽

▽ CONTROL

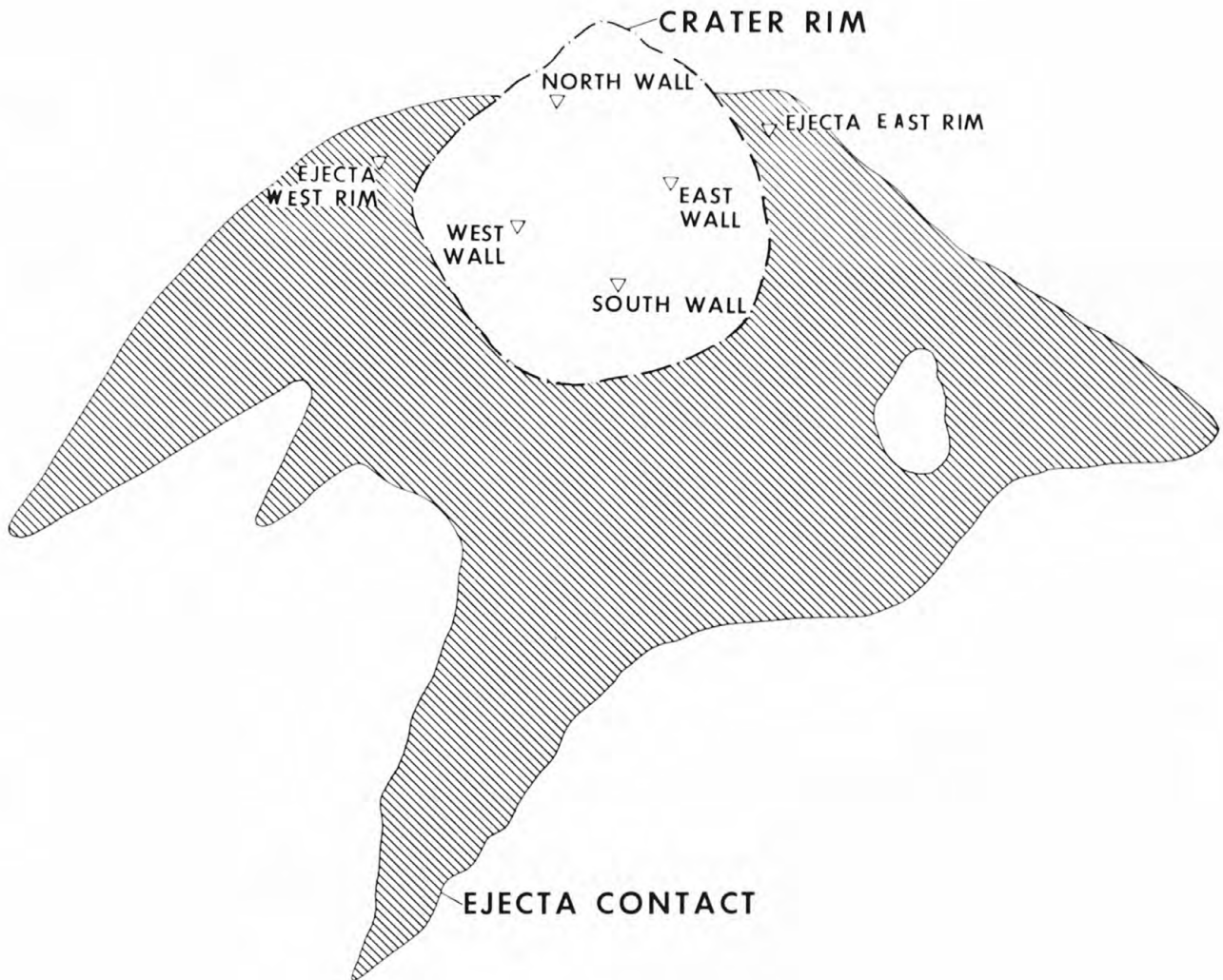


Figure 2. Map of crater 38 showing locations of areas where surface temperatures were measured.  
Scale: 1 inch = 10 feet



Figure 3. Photograph showing thermometers placed in south wall of crater 38.





Figure 4. Photograph showing thermometer placed in north wall of crater 38.



Figure 5. Photograph showing thermometers placed in ejecta of near west rim of crater 38. Note shadows cast by large fragments.



### Description of craters

The general characteristics of missile impact craters have been reported previously (Moore and others, 1964, p. 58-92; Moore, 1966, p. 79-105) and are summarized below. Missile impact craters are depressions produced by ejection of debris as a result of impacts of "inert" missiles with a natural material. For oblique trajectories, the ejecta is deposited symmetrically about the plane of the missile trajectory and is concentrated at right angles to the plane of the trajectory and in "down" trajectory directions (direction in which the missile was going). Very little or no ejecta is deposited "up" trajectory (direction from which the missile came). Materials in and around impact craters may be mapped and classified into seven units: target material, thick ejecta, thin to discontinuous ejecta, tilted and broken target material, shattered target material, slope material, and fallout. Target material is the undeformed material around the craters. Thick ejecta is composed of fragmented target material deposited around the crater in thicknesses exceeding 0.1 to 0.2 foot. Thin to discontinuous ejecta is scattered ejecta around the crater which covers an estimated constant percentage of the surface. Tilted and broken target material is composed of coarsely fractured and rotated target material in the upper crater walls. Shattered material is finely fractured target

material in the "up" trajectory wall. Slope material is talus within the crater usually at the angle of repose. Fallout is fine debris which settles from the air and its distribution is determined by the wind velocity and direction at the time of crater information. Often this unit is so diffuse or similar to the surroundings that it cannot be mapped. Oblique photographs of craters 37 and 38 (figures 6 and 7) show the various map units.

Before proceeding to experimental results, it is noteworthy that materials from lower horizons are brought to the surface during crater formation. For target materials of gypsum, ejecta, fallout, and materials from lower layers are typically whiter and more reflective than the weathered, somewhat brownish, gypsum surface layer of the target material. When a sizeable thickness of alluvium covers a deep layer of gypsum, the ejected debris from the different layers may have a definite pattern around the crater. Proceeding from the "up" trajectory crater rim around the crater to the "down" trajectory rim, materials from progressively deeper horizons are encountered.

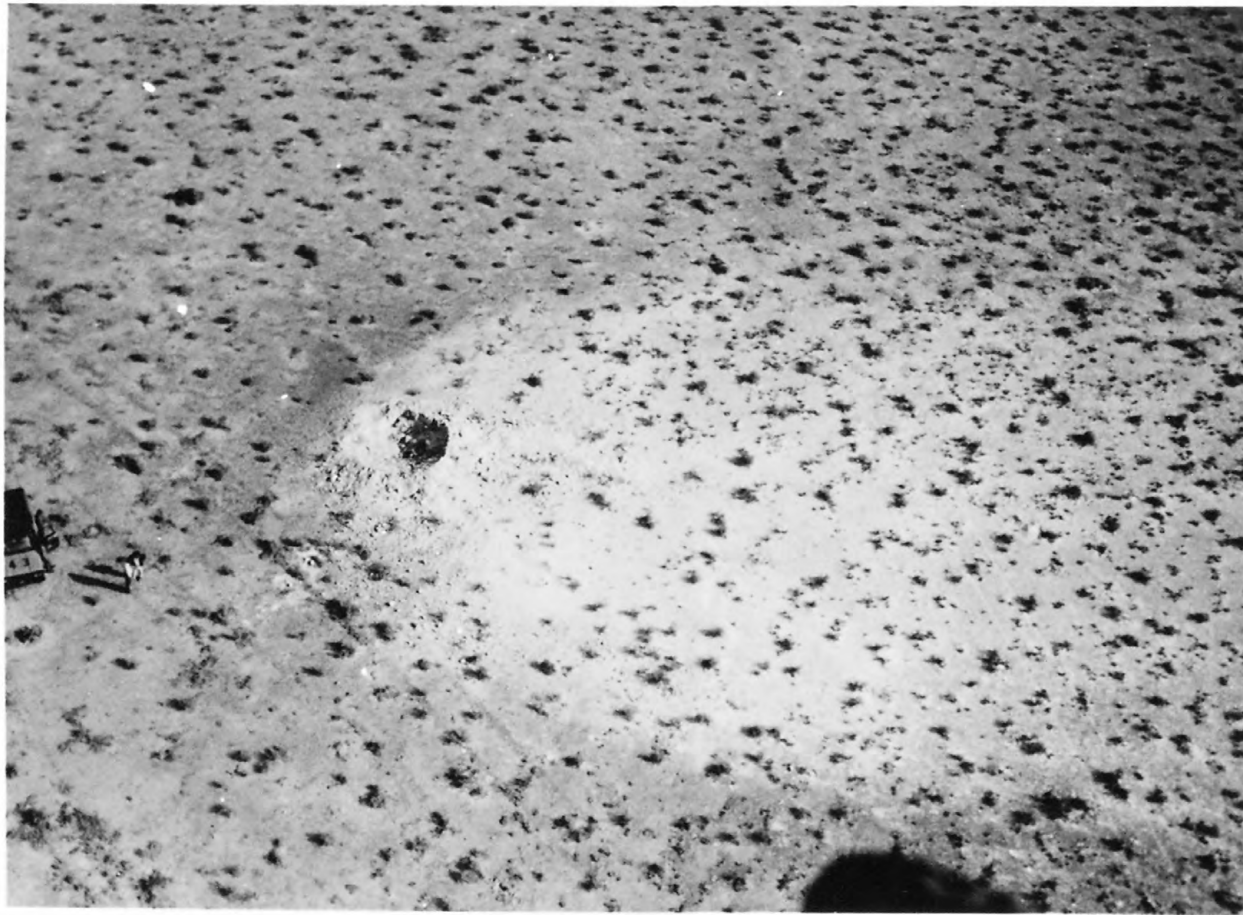


Figure 6. Photograph showing crater 37, ejecta and fallout. Note flat, level terrain.





Figure 7. Photograph showing crater 38, ejecta, and fallout.  
Note fixed dune to right and large variations of  
reflectance of surroundings.

## Experimental results

Comparison of imagery with surface mapping.--Under optimum conditions comparisons between the surface mapping and imagery are exceedingly good. An example of this type of correlation can be seen for crater 18 (fig. 8) which was about 21 months old at the time of the March 1967 flights and a year old at the time of the July 1966 flights. Mapping showed that the crater had typical bilateral symmetry. The thin to discontinuous ejecta was deposited on an  $8^{\circ}$  slope facing  $45^{\circ}$  south-west with an amoeboid pattern. The thick ejecta was fairly close to the rim. This pattern was well shown by the afternoon daylight infrared imagery of July 1966 on which the ejecta was cooler than the surroundings. The crater and ejecta could not be found on the March 1967 daylight or nighttime infrared imagery. Both color and black-white photographic imagery, however, showed the thin to discontinuous ejecta (fig. 8) and the imagery compared well with the map outline. Endeavors to locate the limits of thick ejecta on the photographic imagery were not too successful.

Mediocre correlation of the map and imagery were obtained for crater 28 (fig. 8) which was formed in a gully which sloped in a southerly direction. A "boomerang" shape for the thin to discontinuous ejecta appeared on the surface map as well as the imagery but

Figure 8. Comparisons between surface maps and imagery for craters 18 and 28. Symbols and number indicate origin of figure in framelets:

M -surface map outline, IR - infrared imagery, BW - black and white photographic imagery, CI - color photographic imagery. Dates in map outline framelet indicate time of crater formation; dates in image framelets indicate time of imagery. Scales approximately 1 inch = 120 feet



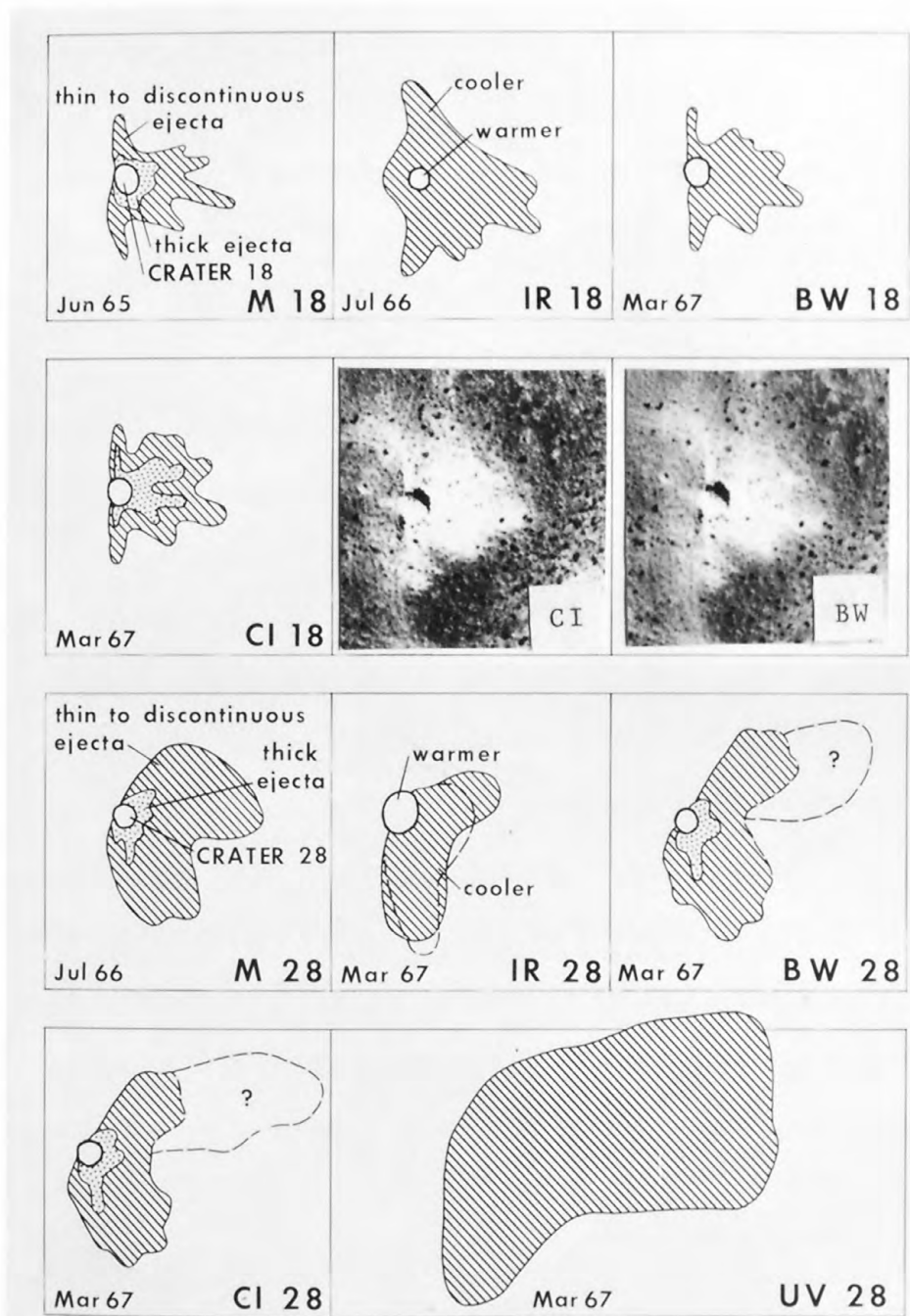


Figure 8.

did not correlate in details as to shape and size. In contrast with the July 1966 daylight infrared imagery on which the crater could not be separated from the ejecta, the March 1967 daylight infrared image shows a warm spot in the crater and the ejecta which is only slightly cooler than the surroundings. Limits of thick ejecta estimate on the photographic imagery correlates reasonably well with that mapped.

Map and image correlations for crater 28 (fig. 9) are poor and only reasonable agreement is obtained for the thick ejecta. The ejecta was deposited on a northerly facing slope near the apex of a fixed dune.

Correlations between the map and imagery for crater 30 are quite good, even for the ultraviolet image (see fig. 9). Daylight infrared imagery show essentially the same pattern for both the July 1966 and March 1967 flights. As might be expected, the daylight infrared image obtained when crater 30 was a few hours old shows more detail than the infrared image when it was eight months old. Here again, the daylight infrared imagery shows a warm spot within the crater for the later imagery whereas no such warm spot is present on the earlier imagery. The ejecta for both daylight infrared images are relatively cooler than the surroundings. The crater was not detected on the night-time infrared imagery. Correlation between photographic imagery and the map outline can be seen to agree

Figure 9. Comparisons between surface maps and imagery for craters 29 and 30. Symbols and numbers indicate origin of figure in framelets:

M - surface map outline, IR - infrared imagery, BW - black and white photographic imagery, CI - color photographic imagery. Dates in map outline framelets indicates time of crater formation; dates in image framelets indicate time of imagery. Crater 29 was produced in July 1966. Scales approximately 1 inch = 120 feet. Photographs reproduced from color imagery.



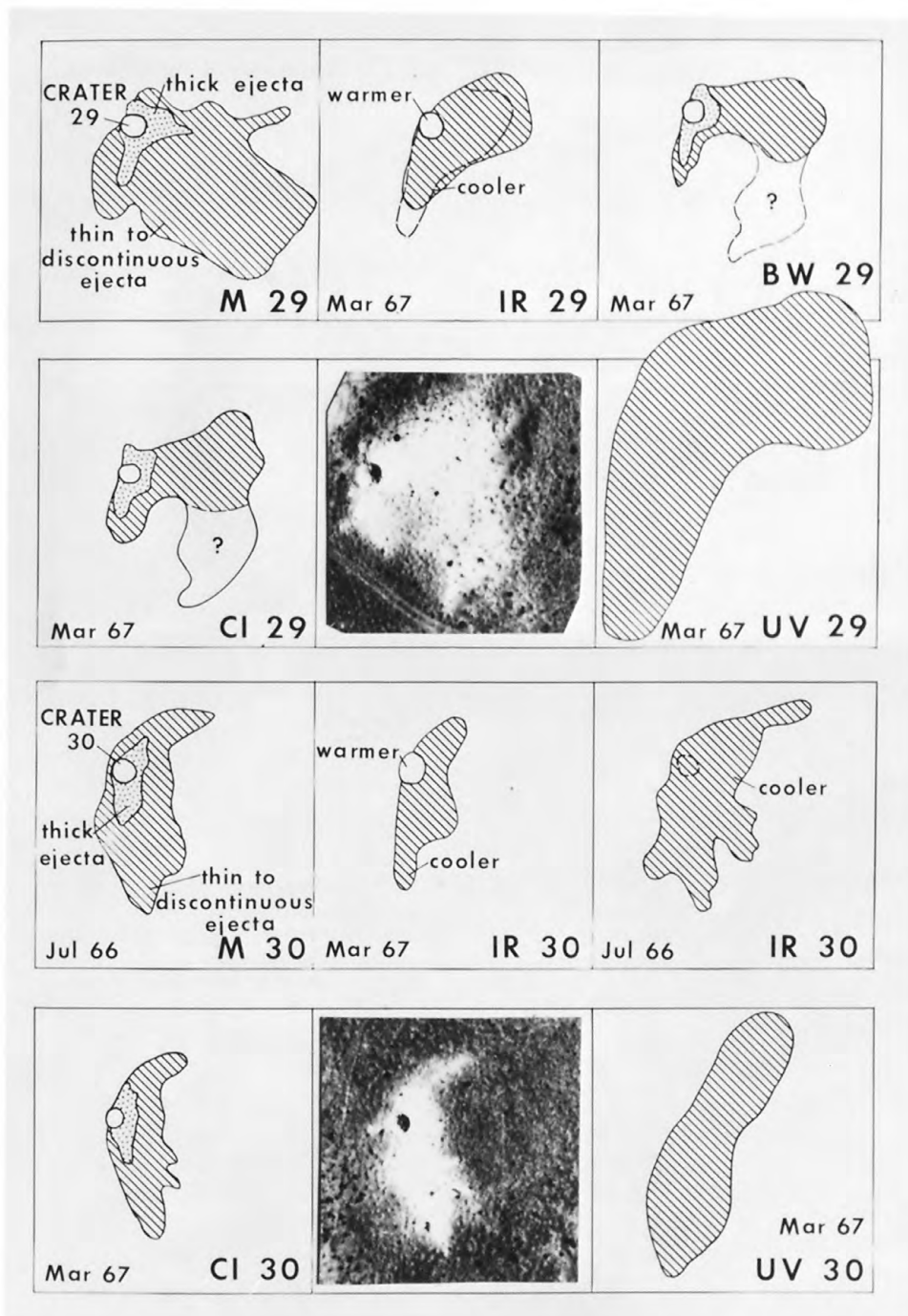


Figure 9.

well. Ultraviolet images for crater 30 agree better with the map outline than all previous images. Ejecta from this crater was deposited on a relatively flat surface.

Photographic imagery of crater 36 (fig. 10) shows the distribution of ejecta from a lower layer of gypsum exceedingly well. The exposures of the ejected white gypsum from the lower layer are distributed symmetrically about the plane of the missile trajectory and closer to this plane than ejecta from the upper layers. Exposures of gypsum ejecta from the lower layer intersect the crater rim near the middle, whereas ejecta of alluvium from the upper layer intersect the crater rim along the "up" trajectory rim. Part of the crater was warm and part of the ejecta was cool in the daylight infrared imagery. The ejecta and crater were not found on the night-time infrared imagery.

Crater 35 was not surface mapped because of possible interference with a geophysical experiment. However, the photographic imagery shows (fig. 10) how the appearance of the ejecta from a deep lower layer of gypsum appears. Crater 35 excavated a small amount of gypsum from a deeper layer than that for crater 36. The imagery shows this where only scattered and isolated exposures of gypsum can be seen. Although the ejecta was not seen in the daylight infrared imagery, the crater appeared as a relatively warm spot.

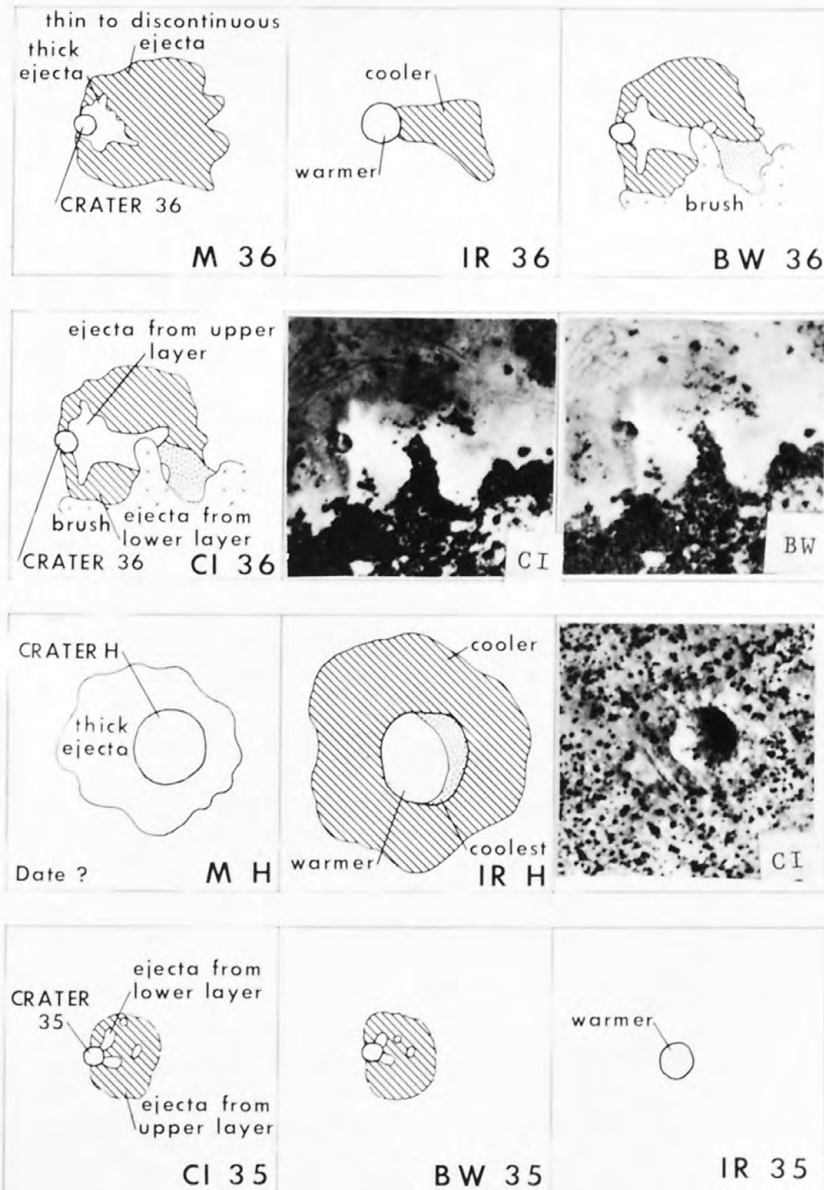


Figure 10. Comparisons between surface maps and imagery for craters 36, H, and 35. All craters formed in March 1967 except crater H. All imagery obtained March 1967. Scales approximately 1 inch = 120 feet



Crater H (fig. 10) was at least several years old at the time of flight and is the largest crater imaged. Partly because of its large size, topographic effects on daylight infrared imagery are well illustrated by this crater. The sunlit wall of the crater appeared warmer than the surroundings and the ejecta; whereas, the shaded wall was cooler than the ejecta and the surroundings. The ejecta from this crater, which is relatively hummocky and rough in detail, appeared cooler than the surroundings. Ejecta from other older large craters with smooth ejecta blankets did not show well on the daylight infrared imagery although sunlit and shaded crater walls did.

All imagery for crater 37 is outstanding as might be expected because the ejecta and fallout were deposited on flat nearly level terrain and the imagery was obtained within a few days after the crater was produced. As a result of its location in flat, level terrain, the imagery actually produce better results than surface mapping in delineating the fallout. In addition, the boundary of the thin to discontinuous ejecta is well shown by the infrared and photographic imagery. Ultraviolet imagery shows the fallout pattern quite well. (figures 11 and 12).

For crater 37 the effects of both the missile trajectory and the wind velocity and direction at the time of impact on the ejecta and fallout distributions can be seen. The local wind direction was about  $45^{\circ}$  from the direction of missile travel and this fact is shown in the

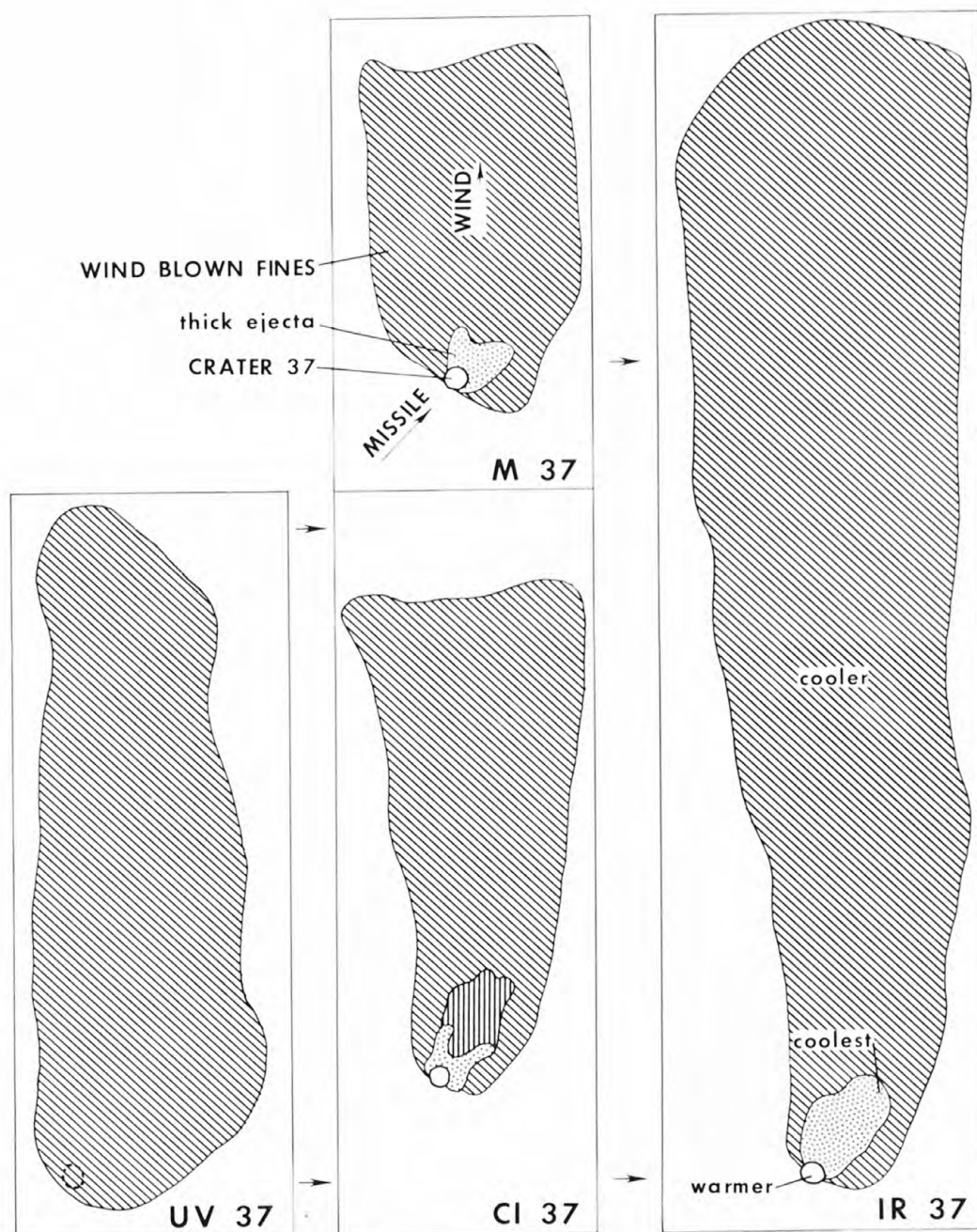


Figure 11. Comparisons between surface map and imagery for crater 37. Imagery obtained March 1967. Arrows on map show trace of path of missile and wind direction. Scales approximately 1 inch = 120 feet

Figure 12. Color (upper) and black-white (lower) imagery of crater 37, ejecta and fallout. Trace of path of missile subparallel to white strip of sheeting. Smaller craters, ejecta, and fallout produced by explosives used for seismic studies. Trucks may be seen to right of crater. Note uniform reflectance of surroundings. Scales approximately 1 inch - 120 feet.

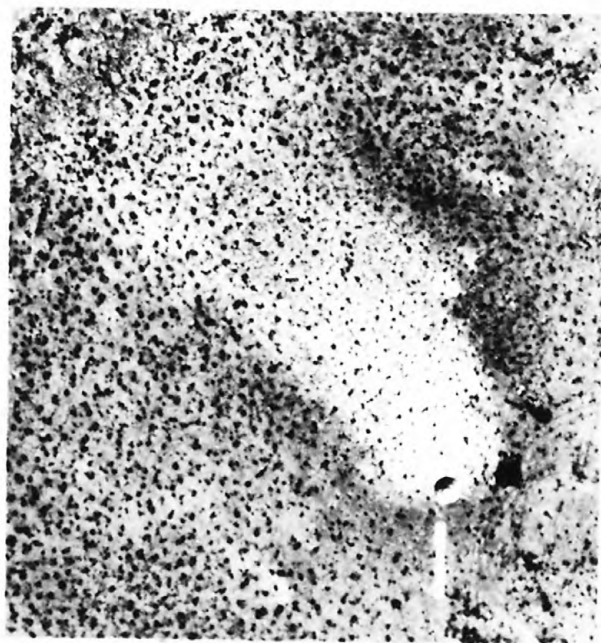
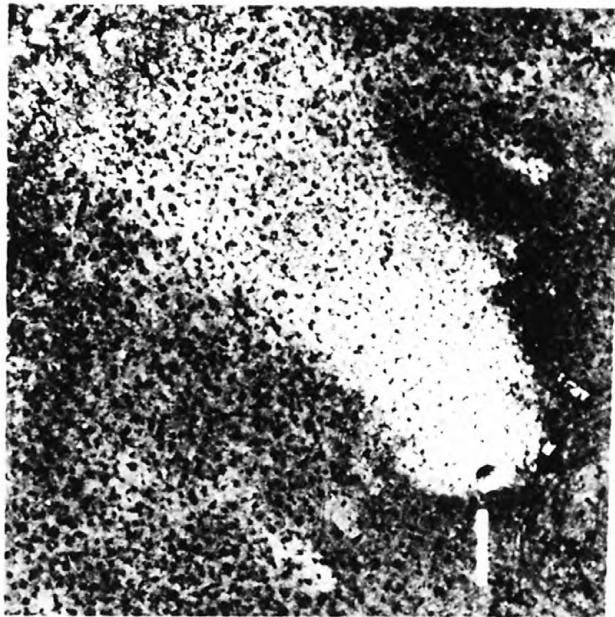


Figure 12



imagery by the distribution of the fallout which is elongate parallel to the wind direction. In contrast, the thin to discontinuous ejecta and thick ejecta are elongate parallel to the direction of travel of the missile. It should be noted--however, that the length of the fallout pattern for the daylight infrared image may be due to scale distortion of the infrared image.

Results of the imagery of crater 38 (figs. 13 and 14), which was produced at the same time as crater 37, are not as good as those of crater 37. Crater 38 is at the northern base of a fixed dune so that part of the ejecta and fall out were deposited on a northerly facing slope. In addition, local variations in color and reflectivity of the surroundings are extreme; thereby making delineation of contacts on the photographic imagery difficult to impossible in places. Some elements of the map and imagery correspond reasonably well such as the thick ejecta boundaries and parts of the contact between thin to discontinuous ejecta and the surroundings. Again, part of the crater wall was relatively warmer and the ejecta relatively cooler than the surroundings on the daylight infrared imagery. Like all previous craters, the ejecta and crater were not seen on the night-time infrared imagery.

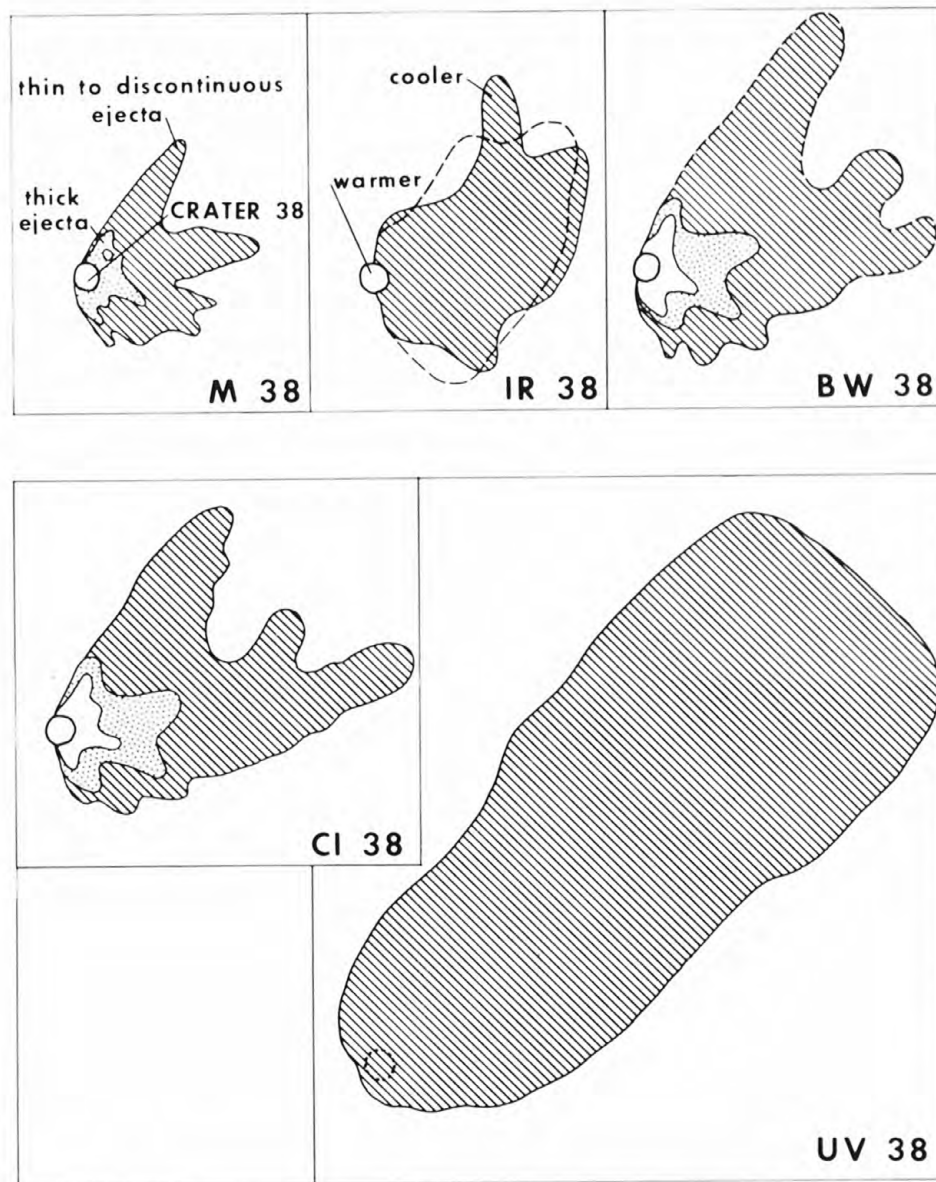


Figure 13. Comparisons between surface map and imagery for crater 38. Crater formed March 1967. Scales approximately 1 inch = 120 feet

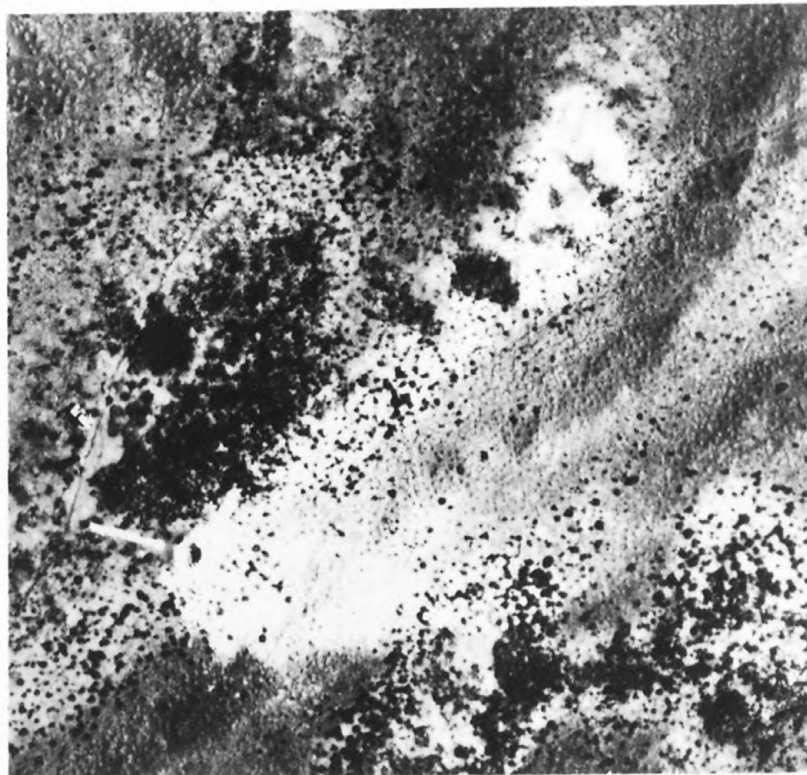


Figure 14. Color image of crater 38, ejecta and fallout. Trace of path of missile subparallel to white strip of sheeting. Note fixed dune along diagonal from lower left to upper right. Note large variations in reflectance of surroundings. Scale approximately 1 inch = 120 feet.

In summary, most of the craters and their ejecta were detected by the imagery obtained by the NASA aircraft. For daylight infrared imagery, part of the craters were warmer than the surroundings whereas the ejecta were cooler. The craters were not detected by the night-time infrared imagery. Ultraviolet imagery detected the ejecta and fallout when they were composed of reflective unweathered gypsum. The photographic imagery also detected the reflective gypsum ejecta and fallout.

The best imagery was obtained for fresh young craters on flat, level ground with little color and reflective variations. Large variations in topography, color, and reflectance of the surroundings have profound effects on the imagery.

Comparison of infrared imagery and measured temperatures.--

Temperatures obtained with the Barnes Radiometer agreed with the infrared imagery for the corresponding times of flight. During the morning both radiometer and infrared imagery indicated the ejecta was cooler than the surroundings and sunlit parts of the crater walls were warmer than the surroundings. During the night-time flight, differences in temperatures were substantially less than during the daylight flight. This is reflected in the night-time infrared imagery on which the craters and their ejecta were not seen.



Data on temperatures for craters 36 and 38 (figs. 15, 16, and 17) show the effects of time of day, local topography, depth, and the map units. Surface temperatures of relatively level areas are low in the early morning; but, rapidly rise to a peak near or later than 12:00 after which they rapidly drop. Subsurface temperatures were generally less than surface temperatures during the late morning and afternoon but they increased until they were higher by sundown. In general, subsurface temperatures decreased with increasing depth and the magnitudes of temperature changes were smaller for larger deposits.

Effects due to topography are shown by differences between both surface temperatures and subsurface temperatures of the north and south walls. North wall temperatures were higher than those of the south wall during the sunlit hours. In addition, west wall surface temperatures reach a maximum in the morning and east wall temperatures reach a maximum in the afternoon. Apparently topographic effects also apply to the surroundings (control) and ejecta because north wall temperatures in the morning exceed those of both the surroundings (control) and ejecta- especially in the morning. South wall subsurface temperatures taken for crater 36 a few hours and less after impact were anomalously high because of heat generated by the impact.

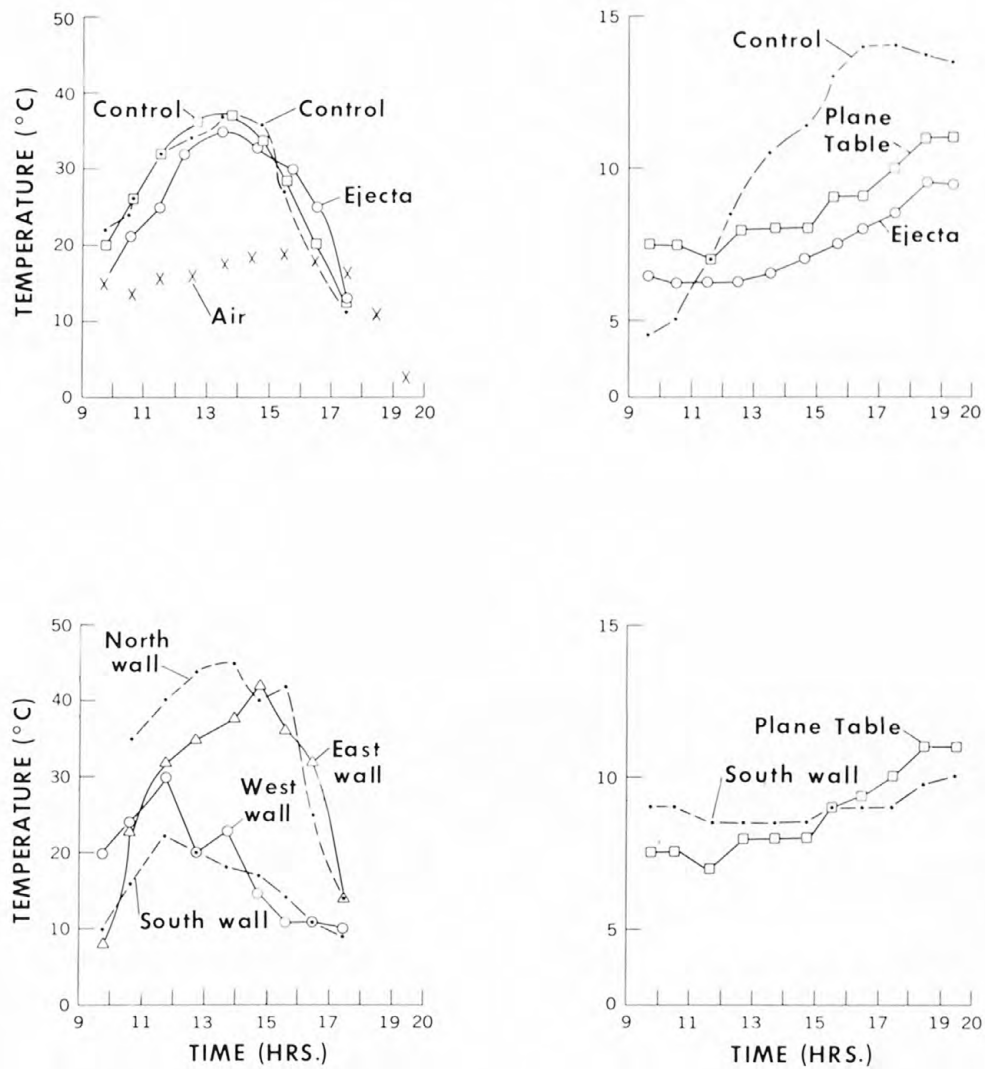


Figure 15. Time-temperature variations for crater 36. Surface temperature to left, subsurface temperatures to right. Data collected 7 March 1967.

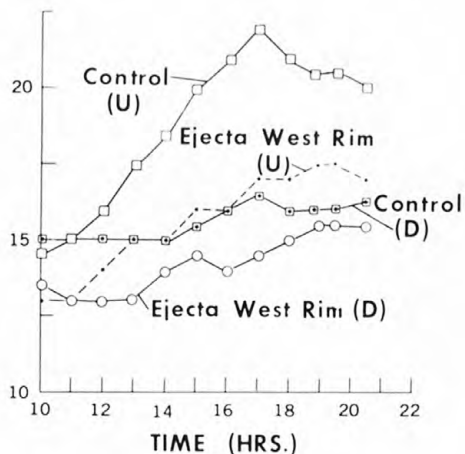
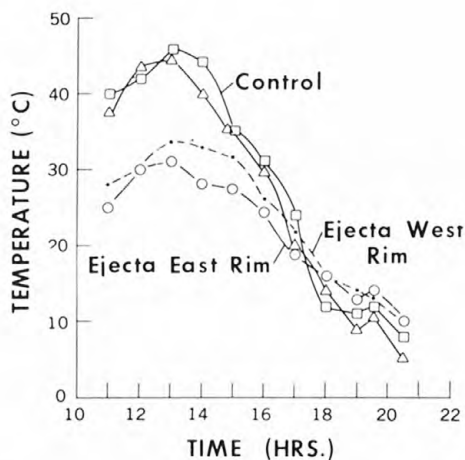
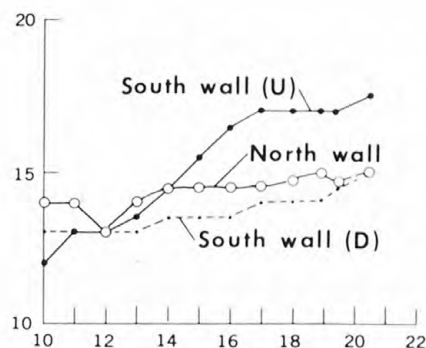
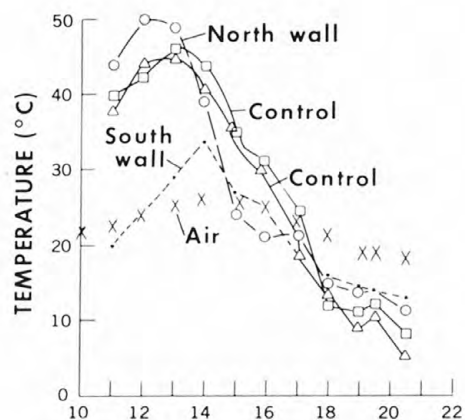


Figure 16. Time-temperature variations for crater 38. Surface temperatures to left, subsurface temperatures to right. Data collected 14 March 1967. Time of remote imaging flight was 19:45-20:00

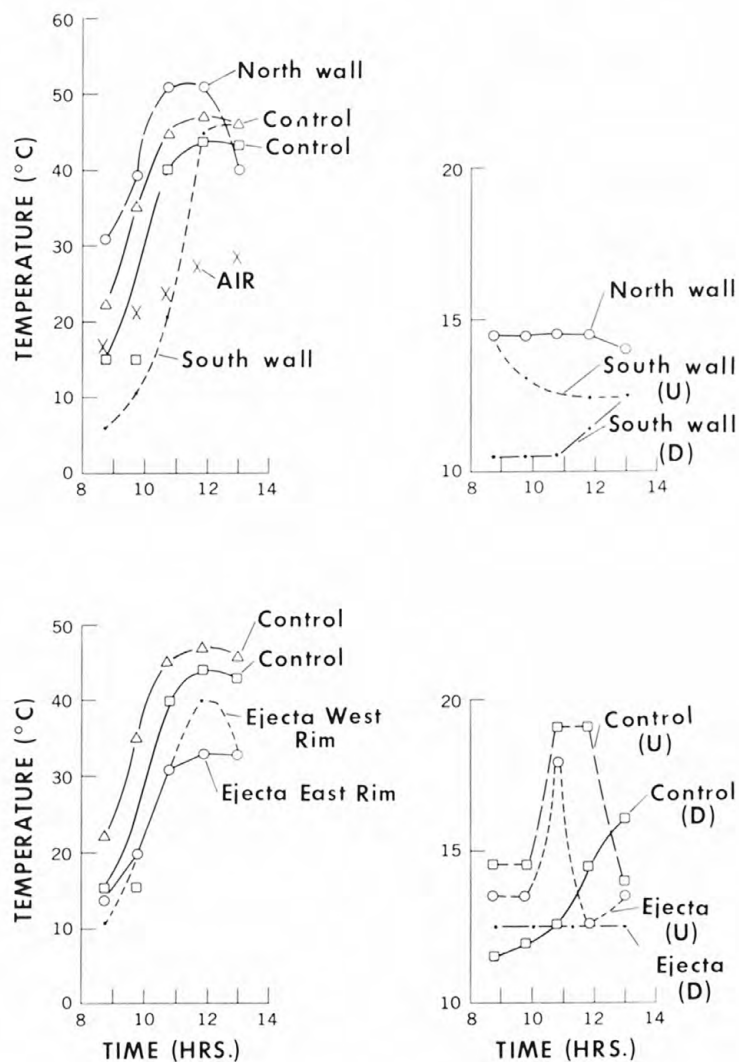


Figure 17. Time temperature variations for crater 38. Surface temperatures to left, subsurface temperatures to right. Data collected 15 March 1967. Time of imaging flight was about 08:00.



Temperatures of the map units: 1) target material or surroundings (control) and 2) ejecta differ throughout the day. Ejecta surface temperatures are lower than those of the surroundings during the morning but they are nearly the same by late afternoon. There are corresponding differences in subsurface temperatures. Ejecta subsurface temperatures are generally less than those of the target material or surroundings (control).

In summary, surface temperatures of the north wall of the craters were higher than those of the south wall, surroundings, and ejecta during the early part of the day. West wall surface temperatures were higher than the east wall temperature during the morning hours; but this reversed in the afternoon. Ejecta surface and subsurface temperatures were generally lower than those of the surroundings (control stations). The subsurface temperatures of the south wall of crater 36, which were measured a few hours after impact, were anomalously high during the morning.

## Explanation of results

Both topography and reflectance influenced the imagery. The influence of topography on the imagery is clearly shown by the shadows shown on the photographic imagery and warm regions within craters on the infrared imagery. The influence of reflectance is clearly shown by white, bright images on the ultraviolet imagery, photographic imagery, and the relatively cold ejecta shown on the infrared imagery.

Although topographic influences are more profound within the craters where sunlit and shaded slopes may be identified on the appropriate imagery, more subtle influences are present. For example, the imagery of crater 37 was outstanding and the flat, level surrounding surfaces were apparently ideal. In contrast, imagery for crater 38 which was at the base of a north-facing slope was difficult to decipher and crater 18, which was on a south-west sloping surface, did not appear on the early morning infrared imagery of March 1967. Crater 18 and ejecta did, however, show quite well on the early afternoon infrared imagery of July 1966. Comparison of infrared images of craters 28, 29, and 30 show that the craters and ejecta on the simplest and levellest terrain show up the best. Since such topographic influences are present on a large scale, they are probably present at smaller scales. This is evident in figures 3, 4, and 5 where blocks and fragments of debris cast shadows on the surrounding finer grained materials.

Reflectance cannot be neglected because (1) the imagery shows that the reflectance of the ejecta is higher than the surroundings for wavelengths between 0.345-0.355 micron and 0.38-0.78 micron, (2) additional large reflectances for gypsum occur for wavelengths between 0.78 and 6 microns (Hovis, 1966a, 1966b), and (3) for a given reflectance, if shadows were predominant in the ejecta because of small scale relief, the ejecta would appear darker than the surroundings. Thus, the fact that the daylight infrared imagery indicates relatively cool ejecta and fallback may be due chiefly to the reflectance of those materials with none, or minor contributions due to micro relief. Since most of the solar energy occurs in ultraviolet and visible wavelengths, the greater reflection of this energy by the ejecta and the greater absorption of this energy by the surroundings would account for the temperature differences observed during the morning and on the daylight infrared imagery.

### Conclusions

1. Infrared, ultraviolet, and photographic imagery can be useful in delineating ejecta, fallout, and other features associated with missile impact craters. The success of the imagery is dependent on local topography and variations of reflectance of both the surroundings and ejected target materials.
2. Infrared imagery and surface temperature measurements are in agreement and can be accounted for by considering the time, the topography, and relative reflectances of the materials involved.

### Future Studies

Additional ground-based studies should be undertaken to measure the surface and subsurface temperature of the ejecta, crater units, and surroundings to 1) determine better times for night-time flights and 2) obtain the time dependent variations of surface and subsurface temperatures which might be used, in turn, to obtain the thermal inertias of the various materials.

Densitometer studies of the imagery might be undertaken to see if the night-time infrared imagery could possibly contain information not detectible by eye.



## References

- Hovis, W. A., 1966a, Infrared spectral reflectance of some common minerals: Applied Optics, v. 5, no. 2, p. 245-248.
- \_\_\_\_\_ 1966b, Optimum wavelength intervals for surface temperature radiometry: Applied Optics, v. 5, no. 5, p. 815-818.
- Moore, H. J., 1966, Craters produced by missile impact, in Astrogeology Studies ann. prog. rept. July 1, 1965-July 1, 1966, Pt. B, U.S. Geol. Surv. open-file rept.
- Moore, H. J., Kachadoorian, Reuben, and Wilshire, H. G., 1964, A preliminary study of craters produced by missile impacts, in Astrogeologic Studies ann. prog. rept. July 1, 1963-July 1, 1965, Pt. B, U.S. Geol. Surv. open-file rept.
- Moore, H. J., Cummings, David, and Gault, D. E., 1967, Use of infrared imagery and color photography in study of missile impact craters: Earth Resources Survey Program Tech. Letter NASA-75, 6 p., 1 fig.
- NASA, 1966, Natural resources program remote sensing aircraft flight data summary report, NASA 926, CV-240A, Mission 28, prepared by Flight Research Project Branch Aircraft Operations Officer, Flight Crew Operations Directorate, Manned Spacecraft Center, Houston, Texas.
- NASA, 1967, Earth Resources Aircraft Program Flight Summary Report, Mission 43, Manned Spacecraft Center, Houston, Texas, March 17, 1967.









USGS LIBRARY - RESTON



3 1818 00155952 3